

JAIME HORTA RANGEL^{1,2)}, WITOLD BROSTOW^{2,*),} VICTOR M. CASTANO^{1,3)}

Mechanical modeling of a single-walled carbon nanotube using the finite element approach

Summary — An analytical procedure to determine the elastic modulus of a single-walled carbon nanotube of armchair type is presented. The interacting forces between atoms are determined based on potentials derived from quantum mechanics. For the axial stretching, the Morse potential parameters were used, along with the bending potential. The model associates a hexagonal lattice where the nodes correspond to atoms and bars to the links (bonds) between them. The finite element model considers fixed position of one end while the tension forces are applied at the other end. The result of the simulation is the shape of the deformed nanotube and its elastic modulus. The influence of the overall dimensions of the nanotube on the modulus of elasticity was also examined.

Keywords: nanotechnology, carbon nanotubes, computer modeling, bond stiffness, advanced materials.

MECHANICZNE MODELOWANIE JEDNOŚCIENNYCH NANORUREK WĘGLOWYCH METODĄ ELEMENTÓW SKOŃCZONYCH

Streszczenie — W artykule opisano procedurę analityczną wyznaczania modułu sprężystości jednościennych nanorurek węglowych o strukturze fotelowej. Siły oddziaływania między atomami wyrażono za pomocą potencjałów wprowadzonych na gruncie mechaniki kwantowej. Do opisu osiowego rozciągania i zginania użyto potencjału typu Morse'a. Model tworzy heksagonalna siatka, w której węzły odpowiadają atomom, a linie wiązaniem między nimi. Metodę elementów skończonych zastosowano do przedstawienia nanorurki, której jeden koniec jest unieruchomiony, podczas gdy do drugiego końca przyłożone są siły rozciągające. Wynikiem symulacji jest kształt zdeformowanej nanorurki i jej moduł sprężystości. Zbadano również wpływ ogólnych wymiarów nanorurki na moduł sprężystości.

Słowa kluczowe: nanotechnologia, nanorurki węglowe, modelowanie komputerowe, sztywność wiązań, materiały zaawansowane.

Carbon nanotubes (CNTs) were identified in 1991 by Iijima as a graphitic carbon hollow structure resembling elongated fullerenes comprised of interconnected hexagons of carbon atoms spanning the entire surface of the nanotube. The ends have the form of half-dome shaped fullerene molecules as a result of topological defects such as pentagonal and heptagonal defects near the tube ends [1]. The spatial orientation of the hexagons is not fixed, which can lead to „chiral” as well as „achiral” CNT configurations. CNTs can be categorized as single-walled nanotubes (SWNTs) or multi-walled nanotubes (MWNTs) [2].

Knowledge of the mechanical behavior of carbon nanotube composites requires the identification of the elastic properties and fracture as well as the interaction with the matrix phases, of the nanotubes themselves. In turn, the properties of nanotubes depend on their atomic arrangement, whether they are of the zig-zag, the armchair or the chiral type, as well as on their specific dimensions. Nanotubes are the known natural objects most similar to the ideal reinforcing fiber, due to their strength and high aspect ratio.

Generally speaking, carbon nanotubes are graphene sheets rolled into a cylinder [3] (see Figures 1 and 2) and are known to have excellent physical and mechanical properties combined with low density, which make them ideal candidates for composite reinforcements [3, 4]. The usual analytic approach reported in the literature is not unlike the case of conventional fibers, the scale of reinforcement, however, involves changing from microns to nanometers, which represents a wholly different situation. Indeed, the morphology of the nanotubes, at the

¹⁾ State University of Queretaro, Queretaro, Mexico.

²⁾ Laboratory of Advanced Polymers and Optimized Materials, University of North Texas, USA.

³⁾ The National Autonomous University of Mexico, Mexico.

^{*}) Corresponding author: wbrostow@yahoo.com

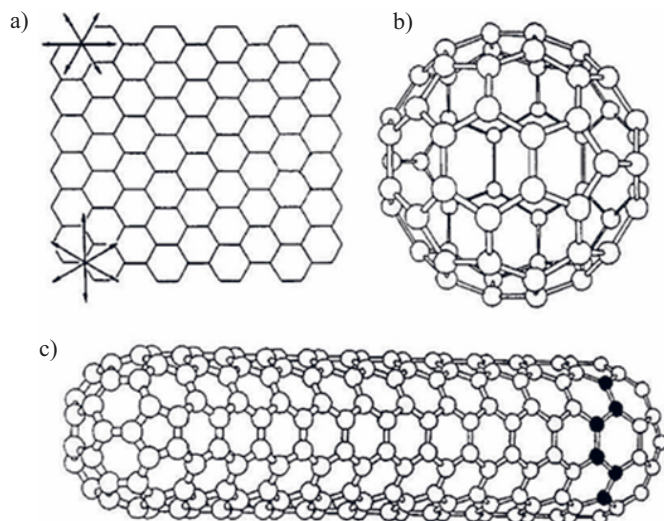


Fig. 1. The structure of: a) graphene sheet, b) fullerene, c) carbon nanotube

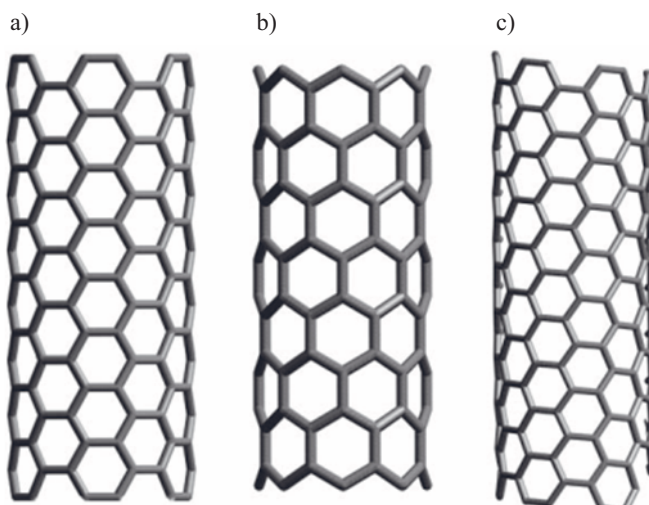


Fig. 2. Basic geometrical arrangements of carbon nanotubes:
a) armchair, b) zig-zag, c) chiral

nanoscale, has been found to generate important changes in the mechanical behavior. For instance, there are reports where the modulus of elasticity depends on the atomic topology, either zig-zag, chiral, etc. Furthermore, the formation of nanotubes in layers also generates significant variations in their final mechanical behavior.

Several experimental studies have determined that the elastic modulus of a nanotube layer is of the order of 1 TPa, that is, orders of magnitude larger than conventional engineering materials, such as steel [4, 5]. Moreover, their structure leads to a high stiffness under tensile stress and remarkable bending properties, with a huge percentage of elongation prior to failure. In the early 80's Kroto *et al.* [6] developed the basics of fullerene chemistry, geometrical structures formed by carbon atoms arranged in hexagonal and pentagonal nanometer rings. Interestingly from the materials science standpoint, fullerenes, carbon nanotubes and graphene share the same

basic chemistry, but their properties are very different and there is a lack of fundamental understanding of the detailed nanostructure-mechanical properties relationship.

Accordingly, the present work is aimed to, first, simulate the mechanical characteristics of arm chair carbon nanotubes, starting from the basic geometry at the nano-scale and, second, to investigate the influence of the dimensions of the nanotubes on their final modulus.

PROPERTIES OF A SINGLE-WALLED NANOTUBE

It has been determined that the distance between carbon atoms (r) is about 0.14 nm [3], while the diameter of the nanotubes varies between 0.4 to 2.5 nm. Maximum resistance to stress has been evaluated around 30 GPa [5]. The axial stretching Morse potential between carbon atoms is defined as follows [7]:

$$F(\Delta r) = 2\beta D_e(1 - e^{-\beta \Delta r})e^{-\beta \Delta r} \quad (1)$$

where: F — the axial force between carbon atoms, $\Delta r = r - r_0$ — stretch which is a difference between current and equilibrium distance between carbon atoms (see Figure 3), D_e — the dissociation energy, β — a constant which describes the potential of atoms interaction.

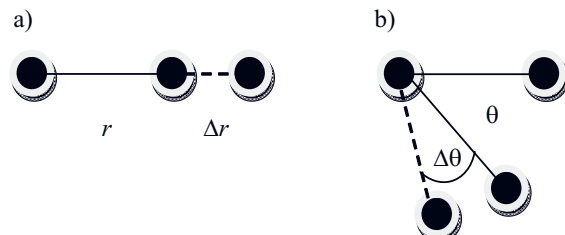


Fig. 3. Interaction between C-C atoms: a) axial stretching,
b) angular stretching

According to Belytschko [8] $\beta = 26.25 \text{ nm}^{-1}$, $D_e = 6.031 \cdot 10^{-10} \text{ N} \cdot \text{nm}$, $r_0 = 0.139 \text{ nm}$. By substituting parameters, we obtain:

$$F = 317 \cdot 10^{-10}(1 - e^{-26.25 \Delta r})e^{-26.25 \Delta r} \quad (2)$$

Figure 4 shows the behavior of bond stiffness. C-C bonds in compression require a big force to stretch them, while the stretch increases, the associated force grows rapidly and tends to infinity (asymptotic value). Figure 5 shows the bond stretching for the range analyzed. On the other hand, according to [7], the momentum-angle relationship under flexion is:

$$M(\Delta\theta) = k_\theta \Delta\theta [1 + 3k_{\text{sextic}}(\Delta\theta)^4] \quad (3)$$

where: M — the angular free (moment) development between carbon atoms, $\Delta\theta = \theta - \theta_0$ — a difference between current and equilibrium bond angle (with $\theta_0 = 2.094 \text{ rad}$), $k_\theta = 0.9 \cdot 10^{-18} \text{ N} \cdot \text{m}/\text{rad}^2$ — the angular force constant of the minimum of the well, $k_{\text{sextic}} = 0.754 \text{ rad}^{-4}$.

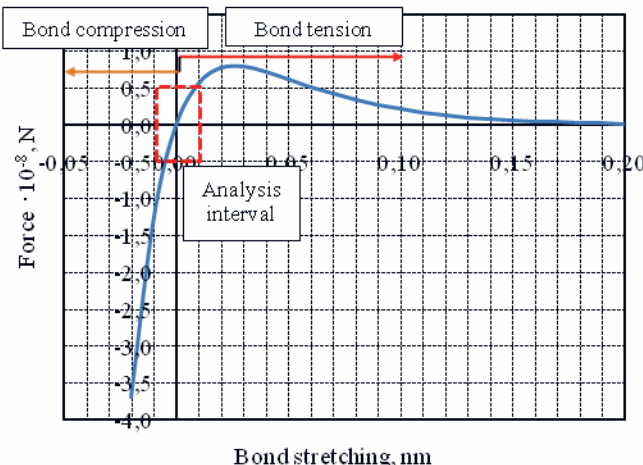


Fig. 4. Force of bond stiffness of carbon atoms

By substituting values of these parameters, to eq. (3) we obtain:

$$M(\Delta\theta) = 0.9 \cdot 10^{-18} \Delta\theta [1 + 2.262 (\Delta\theta)^4] \quad (4)$$

The angle variation $\Delta\theta$ is expressed in radians, Moment M units are in nm. Figure 6 shows a plot obtained according to eq. (4).

EQUIVALENT MECHANICAL STRUCTURAL MODEL

Axial stiffness (K) for bonds in the range indicated is characterized with a lineal approach (Figure 5):

$$K \text{ (axial and angular)} = \frac{\text{difference value forces}}{\text{difference bond stretching values}} \quad (5)$$

For compression load corresponding value is $K_c = 1.1185 \cdot 10^{-6}$ N/nm and for tensile load $K_t = 0.5845 \cdot 10^{-6}$ N/nm. For the range analyzed in this work, the angle dependence of bending stiffness $K_\theta = M/\theta$ is clearly lineal (Fig. 6).

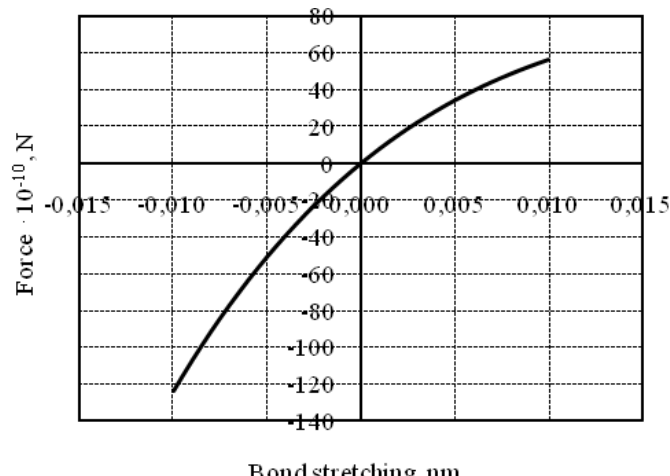


Fig. 5. Force of bond stiffness of carbon atoms – range of the analysis

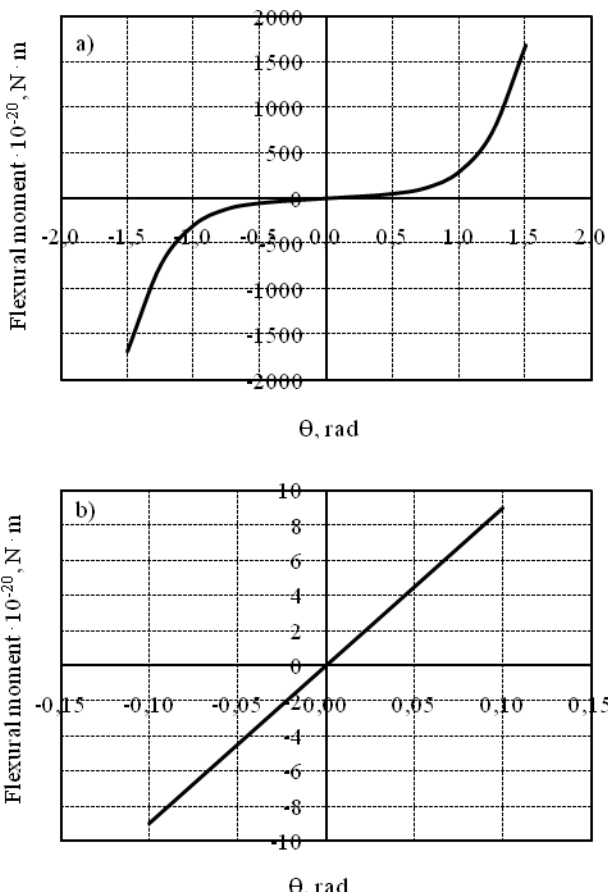


Fig. 6. Relationship between bending flexural moment and bending angle (θ) in wide range (a) and range of current analysis (b)

Substituting values, we obtain: $K_\theta = 0.9 \cdot 10^{-9}$ N · nm. From the perspective of structural mechanics, the bar axial stiffness was assessed by the expression:

$$K_a = AE / L \quad (6)$$

where: A — the cross section area of the bar, E — the modulus of elasticity of the material, L — the length of the bar.

Similarly, the bending stiffness of a beam is evaluated using the formula:

$$K_\theta = 4 EI / L \quad (7)$$

where: I — the moment of inertia of the section.

However, it is necessary to consider that in the expression proposed by Belytshko [8] angle θ is generated with the participation of two links (C-C-C atoms arrangement). So, to ensure the compatibility relation it should be considered a half of the angle θ . Therefore:

$$K_\theta = 2 EI / L \quad (8)$$

Relations (7) and (8) we rewrite considering the below obtained values for K_c , K_t and K_θ :

$$(AE / L)_c = 1.1185 \cdot 10^{-6} \quad (9)$$

$$(AE / L)_t = 0.5845 \cdot 10^{-6}$$

$$(2 EI / L)_\theta = 0.9 \cdot 10^{-9} \quad (10)$$

We assume a circular bars cross section, i.e. $A = \pi d^2/4$ and $I = \pi d^4/64$. By substituting these expressions to eqs. (9) and (10) we obtain:

$$[(\pi d^2 / 4)E / L]_c = 1.1185 \cdot 10^{-6} \quad (11)$$

$$[(\pi d^2 / 4)E / L]_t = 0.5845 \cdot 10^{-6} \quad (12)$$

$$(2 E / L)(\pi d^4 / 64)_0 = 0.9 \cdot 10^{-9} \quad (13)$$

These equations we can write in terms of relations E/L . In the cases of compression and bending, we have:

$$(E / L)_c = 4 \cdot 1.1185 \cdot 10^{-6} / \pi d^2 \quad (14)$$

$$(E / L)_t = 32 \cdot 0.9 \cdot 10^{-9} / \pi d^4$$

Solving eqs. (13) for area and diameter associated by fulfilling both conditions we obtain:

$$\begin{aligned} d_c &= 0.08 \text{ nm} \\ A_c &= 0.005 \text{ nm}^2 \end{aligned} \quad (15)$$

Similarly, for the tension case, we have:

$$\begin{aligned} d_t &= 0.111 \text{ nm} \\ A_t &= 0.00968 \text{ nm}^2 \end{aligned} \quad (16)$$

These results allow us obtaining the stress-strain relationship (Figure 7). We can also obtain the modulus of elasticity E for bonds under compression as well under

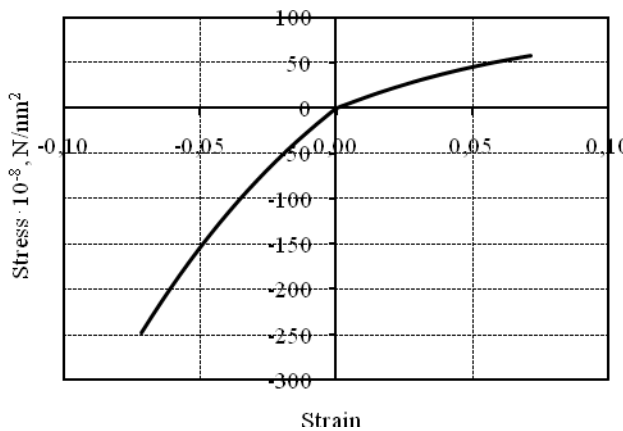


Fig. 7. Stress-strain relationship in the analysis interval — bilinear behavior of modulus E

tension load. The resulting elasticity moduli are as follows:

$$\begin{aligned} E_{tension} &= 913 \cdot 10^{-8} \text{ N/nm}^2 \\ E_{comp} &= 3070 \cdot 10^{-8} \text{ N/nm}^2 \end{aligned} \quad (17)$$

It is possible to simulate other bond deformations, torsion, out-of-plane angle variations, but in agreement with [9–11] these effects are negligible under the small strain conditions applied in this analysis. Van der Walls forces and electrostatic forces were not considered.

To find the elasticity modulus of the whole nanotube we will use the thickness of the equivalent grid nanotube model. This model has two beam areas, one for stretched beams and another for compressed ones (eqs. 14 and 15).

For axial effects Wan and Delale [7] suggest the thickness of the nanotube equal to 0.34 nm, while in bending 0.089 nm. Our case is more associated to axial effects but, when we take the diameter of nanotubes equal to 0.6 nm the wall thickness of 0.34 nm is bigger than the diameter. So we will consider for our purposes the thickness equal to 0.2 nm.

ANALYTICAL MODEL

The analytical model applied is derived from the field equations of continuum mechanics for a linear elastostatic problem [12]:

$$S = 2vE + \lambda trE(I) \quad E = \frac{1}{2}(\nabla u + \nabla u^T) \quad \operatorname{Div} S + b = \rho \ddot{u} \quad (18)$$

where: E — infinitesimal strain tensor; S — stress tensor Piola-Kirchhoff; \ddot{u} — displacement vector; v, λ — Lame constants; I — identity tensor; b — body force; ρ — density.

By applying the variational principle of minimum potential energy [13], we obtain the following matrix equation:

$$\left(\int [B]^T [D] [B] dv \right) \{U\} = \int_A [N]^T \{p\} dA + \int_V [N]^T \{b\} dv + \{P\} \quad (19)$$

where: $[B]$ — matrix of shape function derivatives, $[D]$ — matrix of elastic constants, $[N]$ — shape function matrix, $\{U\}$ — displacement vector, $\{p\}$ — vector of external pressures, $\{b\}$ — vector of body forces, $\{P\}$ — vector of punctual external loads.

The first integral is associated with the deformation energy of the system, while the others are integrals of the load vector. This is the model to study the mechanical behavior of the nanotube, assumed as a beam lattice. The beams are modeled with finite element 3-D beams with 6 degrees of freedom per node.

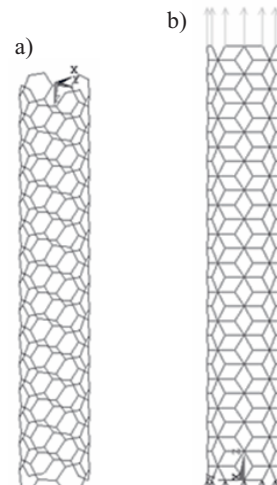


Fig. 8. Lattice model of single-walled carbon nanotube (a) and applied boundary conditions on the nanotube (b)

The atoms are placed in the positions of the nodes and the bars are assigned with the rigidity and dimensions above indicated to generate the lattice (atomistic model) with force (potential) between them. The analysis was performed using the ANSYS modeling program [14], also generating a parametric program in APDL language that allows us to realize all mechanical required analysis. The boundary conditions of the whole nanotube are chosen at the ends, all nodes of one end are restricted in the three main directions. The forces are applied at nodes of the other end of the nanotube (see Figure 8).

The first analysis was performed for an armchair nanotube, with diameter = 1.0 nm and length = 8.0 nm with the aspect ratio $L/D = 8$. The length of the links (bars) is 0.14 nm. According to Ghasemzadeh and Jalalabad [15] we take the poisson's ratio as 0.16. Because it is not possible to know a priori which bars (bonds) experience tension or compression, the analysis was performed in two stages. The first is detecting the kind of stress to which they are subjected. In the second stage, each bar is assigned the appropriate area and modulus of elasticity.

RESULTS AND DISCUSSION

The simulations allow us to observe the behavior under a tensile force for a single-walled carbon nanotube of armchair type. The force applied was increased until it reached a value close to $F_n = 1.0 \cdot 10^{-8}$ N. Figure 9 shows the displacement of the nanotube in nanometers. To evaluate the elastic modulus of the whole nanotube, we take the maximum axial displacement in z direction equal to 0.158 nm. Thus, the deformation is $\varepsilon_z = 0.02$. To evaluate the maximum stress in the nanotube, we divide the final force (F_n) applied by the nanotube cross section area:

$$A_n = \pi D_n t \quad (19)$$

where: D_n — the diameter of nanotube, t — the diameter of nanotube equal to 0.2 nm.

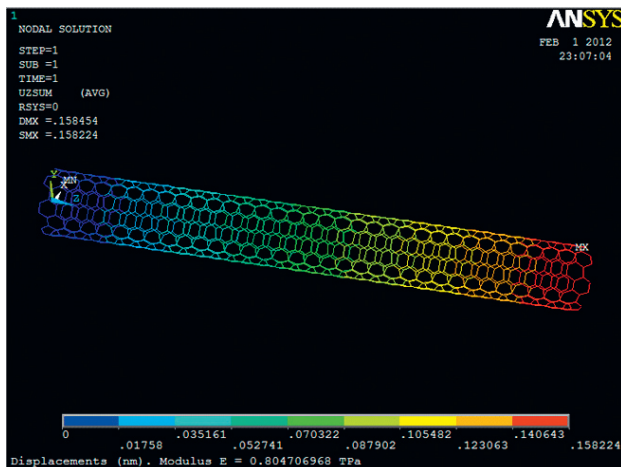


Fig. 9. Deformed shape of a single-walled carbon nanotube — displacements Z-direction in nanometers ($L/D = 8$)

We obtain for this case $A_n = 0.628 \text{ nm}^2$, the modulus of elasticity of the whole nanotube is then obtained as $E = 0.8 \text{ TPa}$, equal to the experimental report obtained by Rossi and Meo [9] for such a nanotube. The analysis of the stress of armchair type nanotube with a bar structural mechanical model turns out to be a practical and efficient approach to evaluate the performance of the nanotube when subjected to different mechanical stresses. Here, we have taken into account tension load, however, it is possible to apply other effects, including the case of dynamical stability, which will be reported separately. The influence of the overall dimensions of this nanotube: diameter and length, was presented in Table 1. It can be observed how the aspect ratio does not affect seriously the mechanical ability of the nanotube, even for high values of the aspect ratio (Figure 10). Figure 11 shows the deformed configuration for $L/D = 30$.

In order to see this influence of diameter on the value of the modulus of the nanotube, we performed a series of analyses with the fixed value of nanotube length of 10.0 nm. We varied the diameter accordingly. The results

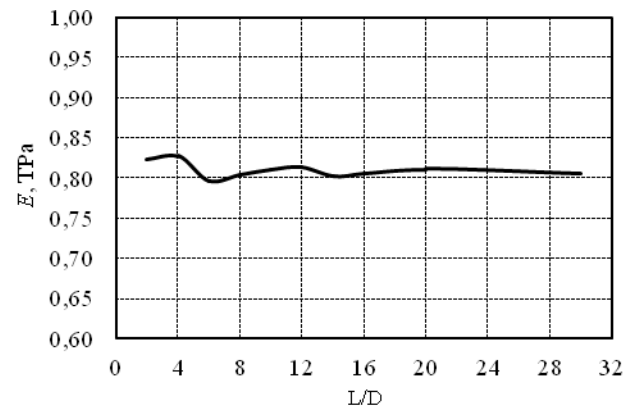


Fig. 10. Effect of aspect ratio (L/D) on modulus E (here D was fixed at 1.0 nm)

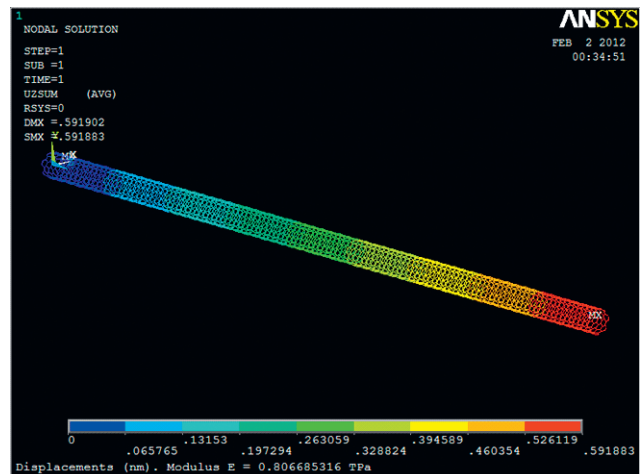


Fig. 11. Deformed shape of a single-walled carbon nanotube of armchair type ($L/D = 30$)

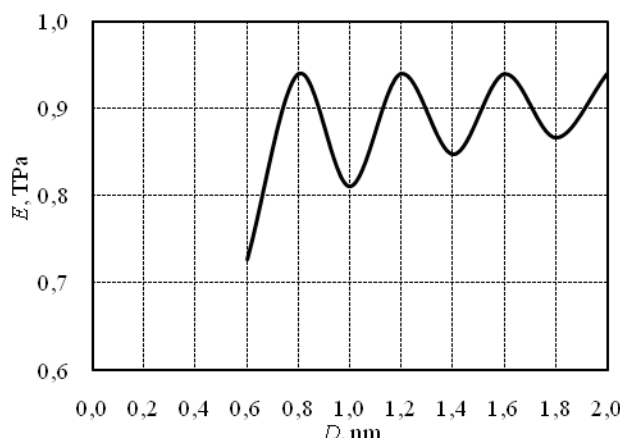


Fig. 12. Modulus E versus diameter of nanotube (D) (length of nanotube was fixed at 10 nm)

are shown in Table 2 and Figure 12. Interestingly, the modulus of elasticity (E) has a decreasing harmonic behavior. For higher values of nanotube diameter, the modulus E approaches 0.9 TPa. Finally, Figure 13 shows the behavior of the nanotube deformed for values $L = 10$ nm and $D = 2.0$ nm.

Table 1. Influence of aspect ratio (L/D) on modulus (E)

L/D	D , nm	L , nm	E , TPa
2	1	2	0.823
4	1	4	0.827
6	1	6	0.796
8	1	8	0.804
10	1	10	0.810
12	1	12	0.813
14	1	14	0.802
16	1	16	0.805
20	1	20	0.811
30	1	30	0.806

Table 2. Influence of diameter of nanotube (D) on modulus (E)

L , nm	D , nm	E , TPa
10	0.6	0.727
10	0.8	0.940
10	1.0	0.810
10	1.2	0.940
10	1.4	0.847
10	1.6	0.940
10	1.8	0.867
10	2.0	0.940

CONCLUDING REMARKS

The outstanding mechanical properties of carbon nanotubes and their potentially massive use as reinforce-

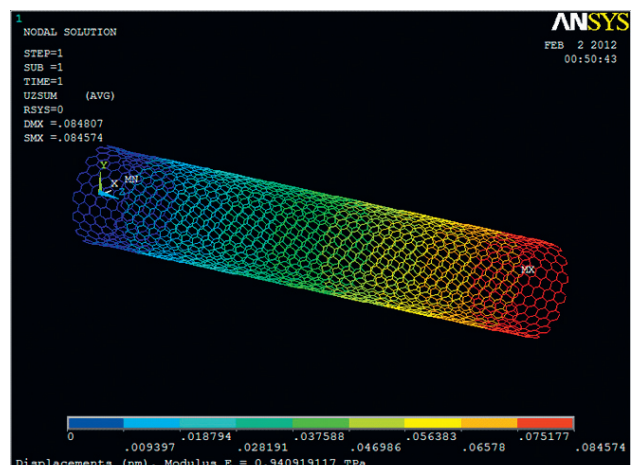


Fig. 13. Deformed shape of a single-walled carbon nanotube of armchair type ($L = 10$ nm, $D = 2.0$ nm)

ing agents, make mandatory a clear understanding of the mechanisms that lead to their unique properties, beginning at the nanoscale level. The simulations we have performed indicate, first, that the lattice model can remarkably reproduce the experimental values reported by various groups and, second, that the mechanical properties seem to be a scalable factor of these fascinating materials. The investigations concerning dynamic behavior of such systems, by using the same approach reported herein, is currently under way and will be reported separately.

REFERENCES

- Li Lingyu, Li Bing, Hood M. A., Li Ch. Y.: *Polymer* 2009, **50**, 953.
- Harris P. J.: „Carbon nanotubes and related structures”, Cambridge University Press 1999.
- Dresselhaus M. S.: *Annu. Rev. Mater. Sci.* 1997, **27**, 1.
- Terrones M.: *Annu. Rev. Mater. Res.* 2003, **33**, 419.
- Treacy M. M. J., Ebbesen T. W., Gibson J. M.: *Nature* 1998, **381**, No. 20, 678.
- Kroto H. W., Heath J. R., O'Brien S. C., Curl R. F., Smalley R. E.: *Nature* 1985, **318**, 162.
- Wan H., Delale F.: *Mecchanica* 2010, **45**, 43.
- Belytschko T., Xiao S. P., Schatz G. C., Ruoff R. S.: *Phys. Rev. B: Condens. Matter.* 2002, **65**, 235 430.
- Rossi M., Meo M.: *Compos. Sci. Technol.* 2009, **69**, 1394.
- Govindjee S., Sackman J. L.: *Solid State Commun.* 1999, **110**, 227.
- Lu J. P.: *J. Phys. Chem. Solids* 1997, **58**, 1649.
- Gurtin M.: „Continuum Mechanics” Academic Press 1981.
- Cook R. D., Malkus D. S., Plesha M. E.: „Concepts and application of finite element analysis”, John Wiley & Sons Inc., New York 1988.
- Ansys, Inc. Software, ver 11, 2009, Canonsburgh PA, USA.
- Ghasemzadeh H., Jalalabad E. A.: *Int. J. Civil Eng.* 2011, **9**, No. 3, 223.

Received 18 V 2012.